International Journal of GEOMATE, May, 2024 Vol.26, Issue 117, pp.27-34
ISSN: 2186-2982 (P), 2186-2990 (O), Japan, DOI: https://doi.org/10.21660/2024.117.4325
Geotechnique, Construction Materials and Environment

THE TRANSPORT LOAD INFLUENCE ON A REINFORCED TWO-LAYERED TUNNEL LINING

Svetlana Girnis[1], Vitaliy Ukrainets[1], *Viktor Stanevish[1], Larisa Gorshkova[1] and Aylin Akhmetova[1]

[1] Faculty of Architecture and Construction, Toraighyrov University, Kazakhstan

*Corresponding Author, Received: 09 Dec. 2023, Revised: 09 March 2024, Accepted: 16 Feb. 2024

ABSTRACT: Despite significant achievements in the field of tunnel construction, adequate methods for their dynamic calculation under transportation load (loads from moving transport within the tunnel) are still practically nonexistent. Particularly significant challenges arise during the calculation of shallowly embedded tunnels. Using the mathematical modelling method, such a calculation was performed for a tunnel supported by a circular cylindrical homogeneous lining. In the presented work, a shallowly embedded tunnel reinforced with a two-layer lining is considered. When creating the mathematical model, the tunnel is represented as a circular cylindrical two-layer shell located in an elastic half-space. The load-free horizontal boundary of the half-space (ground surface) is parallel to the shell axis. Dynamic equations of elasticity theory in Lamé potentials are used to describe the motion of the internal thick layer of the shell and the surrounding body. The vibrations of the external thin layer of the shell are described by classical shell theory equations. The equations are represented in moving Cartesian and cylindrical coordinate systems associated with a load moving uniformly along the inner surface of the shell. Based on the obtained solution to the problem and numerical experiments, the stress-strain state of the two-layer lining of a shallowly embedded tunnel and the surrounding rock body is investigated under the action of a uniformly moving axisymmetric normal load. It is established that at the ground surface when the lining has a rigid contact with the rock body, the displacements and stresses are lower compared to when the contact is sliding.

Keywords: Tunnel, Elastic half-space, Two-layer shell, Transportation load, Stress-strain state

1. INTRODUCTION

Experimental studies show that when tunnels are subjected to transportation loads, vibrations occur both in the structures themselves and in the surrounding rock body. Exceeding the permissible vibration levels can lead to loss of load-bearing capacity of the structures or render them unsuitable for normal operation. In the case of shallowly embedded structures, similar consequences can affect nearby surface structures. It should be noted that experimental methods for studying vibration processes resulting from transportation loads in these structures require significant financial resources, and in some cases, conducting such experiments may not be feasible. Therefore, there is a need for efficient methods of dynamic analysis based on mathematical models using modern mechanics concepts [1].

When constructing a mathematical model for the study of the dynamics of tunnels under the influence of transportation loads, the design of these structures and their depth of installation are of great importance [2, 3]. Most often, this structure is represented as an infinitely long circular cylindrical homogeneous shell placed within an elastic space (design scheme for deep-seated construction) or an elastic half-space (design scheme for shallow construction). The inner surface of the shell is subjected to a load moving along its axis.

The dynamic behavior of elastic space under the action of a moving load on thick-walled and thin-walled homogeneous shells has been investigated in articles [4, 5], respectively and numerous other works. In the dynamic analysis of shallowly buried tunnels under transportation loads, there is a need to consider the influence of waves that are generated during the movement of the load and are reflected by the Earth's surface (the boundary of the half-space). This makes the calculation more complex. Therefore, the number of publications that can be used for the calculation of shallow tunnels and the study of their dynamic behavior under the action of transportation loads is relatively small and mostly covers recent years, particularly [6 – 14]. Here, as in [4, 5], the design scheme of the tunnel lining is a homogeneous circular cylindrical shell. In the presented paper, the tunnel lining structure is modeled as a circular cylindrical shell, consisting of two concentric layers: a thick inner layer and a thin outer layer. The shell layers are rigidly interconnected. The contact between the shell and the body can be either rigid or sliding.

The study aims to obtain an analytical solution to the problem and to develop computer programs based on it to investigate the dynamics of a shallow tunnel reinforced with a two-layer lining, corresponding to the tunnel model adopted in this paper, under the action of stationary transport loads. The proposed solution is presented in the "Results" section, where the numerical experiment results are also provided and analyzed in the "Discussion" section. The sources used in the solution are highlighted in the "Methods" section. The "Conclusion" section summarizes the

findings of the study, recommending that design organizations use the developed mathematical model of the dynamics of shallowly embedded tunnels in metro and tunnel construction.

2. RESEARCH SIGNIFICANCE

The obtained solution and the developed software package based on it enable the investigation of the dynamics of the rock body and the Earth's surface along the tunnel alignment at different velocities of transport loads. This analysis takes into account the physical and mechanical properties of the materials and dimensions of the structural elements of its lining using mathematical modeling methods. The selection of materials and the thickness of the lining shell layers in the tunnel helps reduce surface vibrations along the alignment, which can negatively impact the seismic stability of nearby buildings and structures.

3. METHODS

The research is based on the method of mathematical modeling [1] using elasticity theory. The tunnel is represented as an infinitely long circular cylindrical two-layer shell located in an elastic half-space parallel to its horizontal boundary. Initially, the load moving uniformly along the inner surface of the shell is assumed to be sinusoidal along the shell axis. The method of partial separation of variables [7, 8] is proposed to solve the problem. The solution for Lamé potentials is given as a superposition of Fourier-Bessel series and Fourier-type contour integrals. Next, the method of decomposition of potentials into plane waves and decomposition of plane waves into series over cylindrical functions is used [7, 8]. Finally, the obtained solution is applied to solve the problem of the action of a moving load on this shell, which is not periodic but can be represented in the form of a Fourier integral.

4. RESULTS

4.1 Problem Formulation and Analytical Solution

Let us consider a homogeneous and isotropic medium in Cartesian (x, y, z) and cylindrical (r, θ, z) coordinate systems having a fixed position in space, which is a linearly elastic half-space (body). The half-space, with a load-free horizontal boundary, contains an infinitely long circular cylindrical cavity with a radius of R_1. The cavity's axis aligns with the z-axis, which runs parallel to the boundary. The x-coordinate axis is perpendicular to the boundary of the half-space: $x \le h$, $h > R_1$ (see Fig. 1).

The cavity is reinforced by a two-layer shell, the inner (supporting) layer of which is a thick elastic shell with a radius of the inner surface R_2. The outer (enclosing) layer is a thin-walled elastic shell with a thickness of h_0 and a radius of the middle surface R_1 (due to the small thickness of h_0, it is assumed that the thin-walled shell contacts the thick shell and the medium along its middle surface). The layers of the shell are rigidly interconnected. The contact between the shell and the body can be either sliding (with bilateral coupling in the radial direction) or rigid.

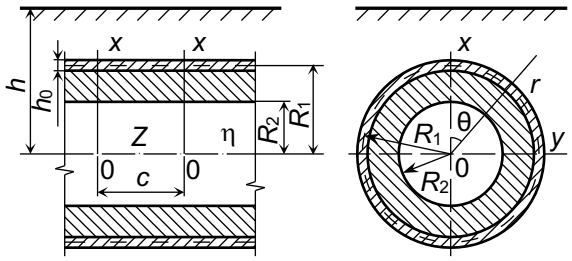

Fig. 1 Two-layer shell in an elastic half-space

The physical and mechanical properties of the materials in the shell layers and the surrounding body are characterised by the following constants: ν_k – Poisson's ratio, μ_k – shift modulus, ρ_k – density ($k = 0, 1, 2$), where index $k = 0$ refers to the enclosing layer of the shell, $k = 1$ – to the body, $k = 2$ – to the supporting layer of the shell.

A load with an intensity P moves along the inner surface of the shell at a constant speed c in the z-axis direction. The load speed is lower than the speed of shear wave propagation in the supporting layer and the body. It is necessary to determine the steady-state response of the shell and the surrounding medium to the given load.

Cartesian (x, y, $\eta = z - ct$) and cylindrical (r, θ, $\eta = z - ct$) coordinate systems moving together with the load are applied to obtain the stationary solution of the problem.

To describe the motion of the half-space ($k = 1$) and the supporting layer of the shell ($k = 2$), the dynamic equations of elasticity theory are used [8, 9]

$$\left(M_{pk}^{-2} - M_{sk}^{-2}\right)\operatorname{grad}\operatorname{div}\mathbf{u}_k + M_{sk}^{-2}\nabla^2\mathbf{u}_k = \partial^2\mathbf{u}_k/\partial\eta^2, \qquad (1)$$

where $M_{pk} = c/c_{pk}$, $M_{sk} = c/c_{sk}$ – the Mach numbers; $c_{sk} = \sqrt{\mu_k/\rho_k}$, $c_{pk} = \sqrt{(\lambda_k + 2\mu_k)/\rho_k}$ – the velocities of shear and expansion-compression wave propagation, $\lambda_k = 2\mu_k\nu_k/(1-2\nu_k)$; ∇^2 – the Laplace operator, $\mathbf{u}_k$ – displacement vectors of the points.

The vibrations of the enclosing layer of the shell will be described by the equations of classical shell theory [7, 13, 14]

$$\left[1 - \frac{(1-\nu_0)\rho_0 c^2}{2\mu_0}\right]\frac{\partial^2 u_{0\eta}}{\partial\eta^2} + \frac{1-\nu_0}{2R^2}\frac{\partial^2 u_{0\eta}}{\partial\theta^2} + \frac{1+\nu_0}{2R}\frac{\partial^2 u_{0\theta}}{\partial\eta\partial\theta} +$$

$$+ \frac{\nu_0}{R}\frac{\partial u_{0r}}{\partial\eta} = \frac{1-\nu_0}{2\mu_0 h_0}\left(q_{\eta 2} - q_{\eta 1}\right),$$

$$\frac{1+\nu_0}{2R}\frac{\partial^2 u_{0\eta}}{\partial\eta\partial\theta}+\frac{(1-\nu_0)}{2}\left(1-\frac{\rho_0 c^2}{\mu_0}\right)\frac{\partial^2 u_{0\theta}}{\partial\eta^2}+$$
$$+\frac{1}{R^2}\frac{\partial^2 u_{0\theta}}{\partial\theta^2}+\frac{1}{R^2}\frac{\partial u_{0r}}{\partial\theta}=\frac{1-\nu_0}{2\mu_0 h_0}(q_{\theta 2}-q_{\theta 1}), \quad (2)$$
$$\frac{\nu_0}{R}\frac{\partial u_{0\eta}}{\partial\eta}+\frac{1}{R^2}\frac{\partial u_{0\theta}}{\partial\theta}+\frac{h_0^2}{12}\nabla^2\nabla^2 u_{0r}+$$
$$+\frac{(1-\nu_0)\rho_0 c^2}{2\mu_0}\frac{\partial^2 u_{0r}}{\partial\eta^2}+\frac{u_{0r}}{R^2}=-\frac{1-\nu_0}{2\mu_0 h_0}(q_{r2}-q_{r1}).$$

Here $R = R_1$; in case $r = R$: $q_{j1} = \sigma_{rj1}$, $q_{j2} = \sigma_{rj2}$ – components of the reaction of the body and the supporting layer of the shell, σ_{rj1}, σ_{rj2} – components of stress tensors in the body and the supporting layer of the shell; u_{0j} – components of displacements of points of the median surface of the enclosing layer of the shell; $j = \eta, \theta, r$.

Let us express the vectors $\mathbf{u}_k$ through the Lamé potentials φ_{jk} ($j = 1, 2, 3$, $k = 1, 2$) [8, 9]

$$\mathbf{u}_k = \operatorname{grad}\varphi_{1k}+\operatorname{rot}(\varphi_{2k}\mathbf{e}_\eta)+\operatorname{rot}\operatorname{rot}(\varphi_{3k}\mathbf{e}_\eta), \quad (3)$$

which, as can be inferred from (1) и (3), satisfy the equations

$$\nabla^2\varphi_{jk}=M_{jk}^2\,\partial^2\varphi_{jk}/\partial\eta^2,\ j=1,2,3,\ k=1,2. \quad (4)$$

Here $\mathbf{e}_\eta$ is the unit vector of η-axis, $M_{1k} = M_{pk}$, $M_{2k} = M_{3k} = M_{sk}$.

The components of the stress tensors σ_{lmk} in the body ($k = 1$) and the supporting layer of the shell ($k = 2$), related to the components u_{lk} of the displacement vectors $\mathbf{u}_k$ by Hooke's law ($l, m = r,\theta,\eta$, $k = 1, 2$; $l, m = x,y,\eta$, $k = 1$), can be expressed through the same potentials φ_{jk}.

Let's first consider the effect of a sinusoidal in η mobile load on the shell

$$P(\theta,\eta)=p(\theta)e^{i\xi\eta},\ p(\theta)=\sum_{n=-\infty}^{\infty}P_n e^{in\theta},$$
$$P_j(\theta,\eta)=p_j(\theta)e^{i\xi\eta},\ p_j(\theta)=\sum_{n=-\infty}^{\infty}P_{nj}e^{in\theta},\ j=r,\theta,\eta, \quad (5)$$

where ξ defines the period $T = 2\pi/\xi$ operating load, $P_j(\theta,\eta)$ – components of the load intensity $P(\theta,\eta)$.

In the steady state, the dependence of all quantities on η takes the form (5), hence

$$\varphi_{jk}(r,\theta,\eta)=\Phi_{jk}(r,\theta)e^{i\xi\eta}.$$

By substituting the last expression into (4), one can obtain

$$\nabla_2^2\Phi_{jk}-m_{jk}^2\xi^2\Phi_{jk}=0,\ j=1,2,3,\ k=1,2, \quad (6)$$

where ∇_2^2 – the two-dimensional Laplace operator, $m_{jk}^2 = 1 - M_{jk}^2$, $m_{1k} \equiv m_{pk}$, $m_{2k} = m_{3k} \equiv m_{sk}$.

Since $c < c_{sk}$, then $M_{sk} < 1$ ($m_{sk} > 0$), $k = 1, 2$. Therefore the solutions of equations (6) can be represented as [8]

$$\Phi_{jk}=\Phi_{jk}^{(1)}+\Phi_{jk}^{(2)},\ j=1,2,3,\ k=1,2, \quad (7)$$

where:

- for the half-space

$$\Phi_{j1}^{(1)}=\sum_{n=-\infty}^{\infty}a_{nj}K_n(k_{j1}r)e^{in\theta},$$
$$\Phi_{j1}^{(2)}=\int_{-\infty}^{\infty}g_j(\xi,\zeta)\exp\left(iy\zeta+(x-h)\sqrt{\zeta^2+k_{j1}^2}\right)d\zeta;$$

- for the supporting layer of the shell

$$\Phi_{j2}^{(1)}=\sum_{n=-\infty}^{\infty}a_{n\,j+3}K_n(k_{j2}r)e^{in\theta},$$
$$\Phi_{j2}^{(2)}=\sum_{n=-\infty}^{\infty}a_{n\,j+6}I_n(k_{j2}r)\,e^{in\theta}.$$

Here $K_n(k_j r)$, $I_n(k_j r)$ – Macdonald functions and modified Bessel functions, $k_{j1}=|m_{j1}\xi|$, $k_{j2}=|m_{j2}\xi|$; $a_{n1},\ldots,a_{n9}$, $g_j(\xi,\zeta)$ – coefficients and functions to be defined, $j = 1, 2, 3$.

In the Cartesian coordinate system, the expressions for the potentials Φ_{j1} (7) will take the form [8]

$$\Phi_{j1}=\int_{-\infty}^{\infty}\left[\frac{e^{-xf_j}}{2f_j}\sum_{n=-\infty}^{\infty}a_{nj}\Phi_{nj}+g_j(\xi,\zeta)e^{(x-h)f_j}\right]e^{iy\zeta}d\zeta, \quad (8)$$

where

$$f_j=\sqrt{\zeta^2+k_{j1}^2},\quad \Phi_{nj}=\left[(\zeta+f_j)/k_{j1}\right]^n,\quad j=1,2,3.$$

Let's express the functions $g_j(\xi,\zeta)$ using the coefficients a_{nj} ($j = 1, 2, 3$). Considering (8), let's use the boundary conditions when $x = h$:

$$\sigma_{xx1}=\sigma_{xy1}=\sigma_{x\eta1}=0.$$

Extracting coefficients of $e^{iy\zeta}$ and equating them to zero, one derives a system of three equations from which one can deduce

$$g_j(\xi,\zeta)=\frac{1}{\Delta_*}\sum_{l=1}^{3}\Delta_{jl}^{*}e^{-hf_l}\sum_{n=-\infty}^{\infty}a_{nl}\Phi_{nl}. \quad (9)$$

The form of the determinants Δ_* and Δ_{jl}^* coincides with the analogous determinants in the case of an unsupported cavity in an elastic half-space and is defined in [1], where it is demonstrated that $\Delta_*(\xi,\zeta)$ does not equal zero when $c < c_R$, with c_R representing the Rayleigh surface wave speed in the half-space.

When $c < c_R$, the relationships (8), taking into account (9), can be rewritten as

$$\Phi_{j1} = \int_{-\infty}^{\infty} \left[\frac{e^{-xf_j}}{2f_j} \sum_{n=-\infty}^{\infty} a_{nj} \Phi_{nj} + \right.$$

$$\left. + e^{(x-h)f_j} \sum_{l=1}^{3} \frac{\Delta_{jl}^*}{\Delta_*} e^{-hf_l} \sum_{n=-\infty}^{\infty} a_{nl} \Phi_{nl} \right] e^{i\gamma\zeta} d\zeta.$$

In the cylindrical coordinate system, at $c < c_R$, the expressions for the potentials Φ_{j1} (7), taking into account (9), will take the form [8]

$$\Phi_{j1} = \sum_{n=-\infty}^{\infty} \left(a_{nj} K_n(k_{j1} r) + b_{nj} I_n(k_{j1} r) \right) e^{in\theta},$$

where $A_{nj}^{ml} = \int_{-\infty}^{\infty} \frac{\Delta_{jl}^*}{\Delta_*} \Phi_{ml} \Phi_{nj} e^{-h(f_l + f_j)} d\zeta$,

$$b_{nj} = \sum_{l=1}^{3} \sum_{m=-\infty}^{\infty} a_{ml} A_{nj}^{ml}.$$

Let us substitute into the components of the stress-strain state (SSS) of the elastic medium ($k = 1$) and the supporting layer of the shell ($k = 2$) represented through the Lame potentials the relations for φ_{jk} found in the cylindrical coordinate system (l, $m = r,\theta,\eta$). Then only the coefficients $a_{n1},\ldots, a_{n9}$ will be unknown in the expressions for displacements u_{lk}^* and stresses σ_{lmk}^* (* indicates that these components correspond to the case of sinusoidal moving load (5) acting on the shell).

Since in the steady state, under the action of a travelling sinusoidal load on the shell, the dependence of all quantities on η has the form (5),

$$u_{0j}(\theta,\eta) = \sum_{n=-\infty}^{\infty} u_{0nj} e^{in\theta} e^{i\xi\eta}, \quad j = r,\theta,\eta. \tag{10}$$

By substituting (10) into (2), one obtains the expression for the n-th term of the expansion

$$\begin{aligned} &\varepsilon_1^2 u_{0n\eta} + \nu_{02} n\xi_0 u_{0n\theta} - 2i\nu_0 \xi_0 u_{0nr} = G_0 (q_{n\eta 2} - q_{n\eta 1}), \\ &\nu_{02} n\xi_0 u_{0n\eta} + \varepsilon_2^2 u_{0n\theta} - 2inu_{0nr} = G_0 (q_{n\theta 2} - q_{n\theta 1}), \\ &2i\nu_0 \xi_0 u_{0n\eta} + 2inu_{0n\theta} + \varepsilon_3^2 u_{0nr} = G_0 (q_{nr2} - q_{nr1}), \end{aligned} \tag{11}$$

where

$\varepsilon_1^2 = \alpha_0^2 - \varepsilon_0^2$, $\varepsilon_2^2 = \beta_0^2 - \varepsilon_0^2$, $\varepsilon_3^2 = \gamma_0^2 - \varepsilon_0^2$, $\xi_0 = \xi R$,

$\alpha_0^2 = 2\xi_0^2 + \nu_{01} n^2$, $\beta_0^2 = \nu_{01}\xi_0^2 + 2n^2$,

$\gamma_0^2 = \chi^2 (\xi_0^2 + n^2)^2 + 2$, $\varepsilon_0^2 = \nu_{01}\xi_0^2 M_{s0}^2$,

$\nu_{01} = 1 - \nu_0$, $\nu_{02} = 1 + \nu_0$, $M_{s0} = c / c_{s0}$,

$c_{s0} = (\mu_0 / \rho_0)^{1/2}$, $\chi^2 = h_0^2 / (6R^2)$, $G_0 = -\frac{\nu_{01} R^2}{\mu_0 h_0}$;

in case $r = R$: $q_{nj1} = (\sigma_{rj1}^*)_n$, $q_{nj2} = (\sigma_{rj2}^*)_n$, $j = \eta, \theta, r$.

Resolving (11) with respect to $u_{0n\eta}$, $u_{0n\theta}$, u_{0nr}, find

$$u_{0n\eta} = \frac{G_0}{\delta_n} \sum_{j=1}^{3} \delta_{\eta j} (q_{nj2} - q_{nj1}),$$

$$u_{0n\theta} = \frac{G_0}{\delta_n} \sum_{j=1}^{3} \delta_{\theta j} (q_{nj2} - q_{nj1}),$$

$$u_{0nr} = \frac{G_0}{\delta_n} \sum_{j=1}^{3} \delta_{rj} (q_{nj2} - q_{nj1}).$$

Here

$\delta_n = \delta_{|n|} = (\varepsilon_1\varepsilon_2\varepsilon_3)^2 - (\varepsilon_1\xi_1)^2 - (\varepsilon_2\xi_2)^2 - (\varepsilon_3\xi_3)^2 +$

$+2\xi_1\xi_2\xi_3$,

$\delta_{\eta 1} = (\varepsilon_2\varepsilon_3)^2 - \xi_1^2$, $\delta_{\eta 2} = \xi_1\xi_2 - \xi_3\varepsilon_3^2$,

$\delta_{\eta 3} = i(\varepsilon_2^2\xi_2 - \xi_1\xi_3)$,

$\delta_{\theta 1} = \delta_{\eta 2}$, $\delta_{\theta 2} = (\varepsilon_1\varepsilon_3)^2 - \xi_2^2$, $\delta_{\theta 3} = i(\varepsilon_1^2\xi_1 - \xi_2\xi_3)$,

$\delta_{r1} = -\delta_{\eta 3}$, $\delta_{r2} = -\delta_{\theta 3}$, $\delta_{r3} = (\varepsilon_1\varepsilon_2)^2 - \xi_3^2$,

$\xi_1 = 2n$, $\xi_2 = 2\nu_0\xi_0$, $\xi_3 = \nu_{02}\xi_0 n$;

for q_{nj1} and q_{nj2} index $j = 1$ corresponding to the index η, $j = 2 - \theta$, $j = 3 - r$.

To determine the coefficients $a_{n1},\ldots, a_{n9}$ one uses the following boundary conditions:

- for sliding contact of the shell with the surrounding body

at $r = R_1$ $u_{r1}^* = u_{r2}^*$, $u_{j2}^* = u_{0j}$, $\sigma_{r\eta 1}^* = 0$, $\sigma_{r\theta 1}^* = 0$,

at $r = R_2$ $\sigma_{rj2}^* = P_j(\theta,\eta)$, $j = r, \theta, \eta$;

- for rigid shell contact with the surrounding body

at $r = R_1$ $u_{j1}^* = u_{j2}^*$, $u_{j1}^* = u_{0j}$,

at $r = R_2$ $\sigma_{rj2}^* = P_j(\theta,\eta)$, $j = r, \theta, \eta$.

By substituting the corresponding expressions into the boundary conditions for the specified type of contact between the shell and the body and equating the coefficients of the Fourier–Bessel series at $e^{in\theta}$, a system of linear algebraic equations is obtained for each value of $n = 0, \pm 1, \pm 2, \ldots$. The coefficients $a_{n1},\ldots, a_{n9}$ can be determined from this system of equations.

Knowing the solution to the problem for the sinusoidal load (5), the response of the shell and the surrounding body to a uniformly moving aperiodic load of the form $P(\theta,\eta) = p(\theta)p(\eta)$ (typical for vehicles) can be found by superposition, using the representation of the load and the SSS components of the half-space and the supporting layer of the shell in the form of Fourier integrals

$$P(\theta,\eta) = \frac{1}{2\pi} \int_{-\infty}^{\infty} P^*(\theta,\xi) e^{i\xi\eta} d\xi = p(\theta)p(\eta) =$$

$$= p(\theta) \frac{1}{2\pi} \int_{-\infty}^{\infty} p^*(\xi) e^{i\xi\eta} d\xi,$$

$$P_m(\theta,\eta) = \frac{1}{2\pi} \int_{-\infty}^{\infty} P_m^*(\theta,\xi) e^{i\xi\eta} d\xi = p_m(\theta)p(\eta) =$$

$$= p_m(\theta) \frac{1}{2\pi} \int_{-\infty}^{\infty} p^*(\xi) e^{i\xi\eta} d\xi;$$

$$u_{lk}(r,\theta,\eta)=\frac{1}{2\pi}\int_{-\infty}^{\infty}u^{*}_{lk}(r,\theta,\xi)p^{*}(\xi)d\xi,$$
$$\sigma_{lmk}(r,\theta,\eta)=\frac{1}{2\pi}\int_{-\infty}^{\infty}\sigma^{*}_{lmk}(r,\theta,\xi)p^{*}(\xi)d\xi. \quad (12)$$

Here $l=r,\theta,\eta$, $m=r,\theta,\eta$, $k=1, 2$.

$$p^{*}(\xi)=\int_{-\infty}^{\infty}p(\eta)e^{-i\xi\eta}d\eta.$$

Any numerical integration method can be used to calculate the displacements and stresses (12), as long as for each value of $n=0,\pm1,\pm2,\ldots\ \Delta_n(\xi,c)\neq0$. Investigations on the determinants $\Delta_n(\xi,c)$ have shown that this condition is satisfied if the speed of the moving load c is less than its critical speeds $c_{(n)*}$ ($c<c_{(n)*}$), which can be lower than the Rayleigh surface wave speed and depend on the number n. Dispersion equations $\Delta_n(\xi, c)=0$ establish these critical speeds at the minima of the respective dispersion curves at $c\sim\xi$. Additionally, it has been demonstrated by calculations that the lowest critical speed takes place when $n=0$ (min $c_{(n)*}=c_{(0)*}$) [7, 8].

4.2 Numerical Experiments

Let us consider a tunnel reinforced with a two-layered steel-concrete lining, buried at a depth of $h=6$ m within a rock body characterized by the following properties: $\rho_1=1{,}5\cdot10^3$ kg/m^3, $\nu_1=0{,}294$, $\mu_1=\mu=1{,}0935\cdot10^8$ Pa. Design parameters for the lining: inner (load-bearing) layer – thick-walled concrete ($\rho_2=2{,}5\cdot10^3$ kg/m^3, $\nu_2=0{,}2$, $\mu_2=1{,}21\cdot10^{10}$ Pa) [15] the shell is 0,5 m thick and the radii of the surfaces $R_1=R=3{,}0$ m, $R_2=2{,}5$ m, the outer (enclosing) layer is thin-walled steel ($\rho_0=7{,}8\cdot10^3$ kg/m^3, $\nu_0=0{,}3$, $\mu_0=8{,}08\cdot10^{10}$ Pa) shell thickness $h_0=0{,}02$ m. The contact between the layers of the lining is assumed to be rigid.

An axisymmetric normal load of intensity q (Pa) moving at a speed $c=100$ m/s along the tunnel exerts a uniform pressure on its lining in the interval $|\eta|\le l_0=0{,}2$ m. The intensity of the load is chosen in such a way that the total load along the entire length of the loading section $2l_0$ was equal to the concentrated normal ring load intensity $P^{\circ\circ}$ (N/m), i.e. $q=P^{\circ\circ}/2l_0$. Numerical investigations of the corresponding dispersion equations for this case have shown that within the subsonic range of speeds, they do not have roots for any contact conditions between the lining and the surrounding rock body.

The names indicated (index k is omitted): $u^{\circ}_r=u_r\mu/P^{\circ}$(m), $\sigma^{\circ}_{rr}=\sigma_{rr}/P^{\circ}$, $\sigma^{\circ}_{\theta\theta}=\sigma_{\theta\theta}/P^{\circ}$, $\sigma^{\circ}_{\eta\eta}=\sigma_{\eta\eta}/P^{\circ}$; $u^{\circ}_x=u_x\mu/P^{\circ}$(m), $u^{\circ}_y=u_y\mu/P^{\circ}$(m), $\sigma^{\circ}_{yy}=\sigma_{yy}/P^{\circ}$, where $P^{\circ}=P^{\circ\circ}$/m (Pa).

Tables 1 – 3 in the xy coordinate plane ($\eta=0$) present the results of calculating the SSS of the supporting layer of the tunnel lining and the rock body. Table 1 provides the values of the SSS components of the inner ($r=R_2$) and outer ($r=R_1$) surface of the lining's supporting layer. Table 2 shows the values of the SSS components at the contact surface of the rock body ($r=R_1$). The values of the SSS components of the ground surface ($x=h$) are presented in Table 3. Figures 2 – 5 illustrate the curves depicting changes in the components of SSS at the ground surface. Curves 1 correspond to rigid contact of the lining with the rock mass, while curves 2 represent sliding contact.

Table 1 Components of the SSS of the supporting layer of the lining in the xy coordinate plane ($\eta=0$)

r	Components of the SSS	|θ|, deg. 0	20	40	60	80	100	120	140	160	180
Rigid contact of the lining with the rock body											
R_2	$u^{\circ}_r\times10$	0.24	0.24	0.23	0.23	0.23	0.23	0.22	0.22	0.23	0.23
	σ°_{rr}	-2.5	-2.5	-2.5	-2.5	-2.5	-2.5	-2.5	-2.5	-2.5	-2.5
	$\sigma^{\circ}_{\theta\theta}$	1.00	1.01	1.01	1.02	1.02	1.02	1.01	1.01	1.00	1.00
	$\sigma^{\circ}_{\eta\eta}$	-4.33	-4.33	-4.32	-4.32	-4.33	-4.33	-4.33	-4.33	-4.33	-4.33
R_1	$u^{\circ}_r\times10$	0.21	0.21	0.20	0.20	0.20	0.20	0.19	0.19	0.20	0.20
	σ°_{rr}	-0.15	-0.15	-0.15	-0.16	-0.16	-0.16	-0.16	-0.16	-0.16	-0.16
	$\sigma^{\circ}_{\theta\theta}$	2.04	2.03	2.03	2.02	2.02	2.01	2.01	2.02	2.02	2.02
	$\sigma^{\circ}_{\eta\eta}$	1.48	1.48	1.47	1.47	1.46	1.46	1.46	1.46	1.6	1.46
Sliding contact of the lining with the rock body											
R_2	$u^{\circ}_r\times10$	0.24	0.24	0.24	0.23	0.23	0.23	0.22	0.22	0.23	0.23
	σ°_{rr}	-2.5	-2.5	-2.5	-2.5	-2.5	-2.5	-2.5	-2.5	-2.5	-2.5
	$\sigma^{\circ}_{\theta\theta}$	1.02	1.02	1.03	1.04	1.04	1.03	1.03	1.02	1.01	1.01
	$\sigma^{\circ}_{\eta\eta}$	-4.35	-4.34	-4.34	-4.34	-4.34	-4.34	-4.34	-4.35	-4.35	-4.35
R_1	$u^{\circ}_r\times10$	0.21	0.21	0.21	0.20	0.20	0.20	0.19	0.19	0.20	0.20
	σ°_{rr}	-0.15	-0.15	-0.15	-0.15	-0.15	-0.15	-0.15	-0.15	-0.15	-0.15
	$\sigma^{\circ}_{\theta\theta}$	2.06	2.06	2.05	2.04	2.04	2.04	2.04	2.04	2.05	2.05
	$\sigma^{\circ}_{\eta\eta}$	1.53	1.53	1.52	1.51	1.51	1.50	1.50	1.50	1.50	1.51

Table 2 Components of the SSS of the contact surface of the rock body ($r = R_1$) in the xy coordinate plane ($\eta = 0$)

r	Components of the SSS	|θ|, deg.									
		0	20	40	60	80	100	120	140	160	180
Rigid contact of the lining with the rock body											
R_1	$u^\circ_r \times 10$	0.21	0.21	0.20	0.20	0.20	0.20	0.19	0.19	0.20	0.20
	$\sigma^\circ_{rr} \times 10$	-0.41	-0.42	-0.43	-0.44	-0.44	-0.44	-0.44	-0.44	-0.44	-0.44
	$\sigma^\circ_{\theta\theta} \times 10$	0.05	0.05	0.04	0.04	0.04	0.04	0.04	0.04	0.04	0.04
	$\sigma^\circ_{\eta\eta} \times 10$	0.0	0.0	-0.01	-0.01	-0.01	-0.01	-0.01	-0.01	-0.01	-0.01
Sliding contact of the lining with the rock body											
R_1	$u^\circ_r \times 10$	0.21	0.21	0.21	0.20	0.20	0.20	0.19	0.19	0.20	0.20
	$\sigma^\circ_{rr} \times 10$	-0.33	-0.34	-0.36	-0.37	-0.37	-0.38	-0.37	-0.38	-0.38	-0.38
	$\sigma^\circ_{\theta\theta} \times 10$	-0.04	-0.04	-0.03	-0.03	-0.03	-0.03	-0.03	-0.04	-0.04	-0.04
	$\sigma^\circ_{\eta\eta} \times 10$	-0.34	-0.34	-0.34	-0.34	-0.34	-0.34	-0.34	-0.34	-0.34	-0.34

Table 3 Components of the SSS at the ground surface ($x = h$) in the xy coordinate plane ($\eta = 0$)

Components of the SSS	|y|, m								
	0.0	0.4	0.8	1.2	1.6	2.0	2.4	2.8	3.2
Rigid contact of the lining with the rock body									
$u^\circ_x \times 100$	0.73	0.73	0.71	0.69	0.66	0.63	0.59	0.56	0.53
$u^\circ_y \times 100$	0.0	0.04	0.07	0.10	0.12	0.13	0.14	0.15	0.14
$\sigma^\circ_{yy} \times 100$	0.44	0.43	0.40	0.36	0.31	0.25	0.19	0.14	0.10
$\sigma^\circ_{\eta\eta} \times 100$	0.72	0.72	0.70	0.67	0.63	0.58	0.54	0.50	0.46
Sliding contact of the lining with the rock body									
$u^\circ_x \times 100$	0.89	0.89	0.87	0.84	0.81	0.77	0.72	0.68	0.64
$u^\circ_y \times 100$	0.0	0.04	0.08	0.11	0.14	0.16	0.17	0.17	0.17
$\sigma^\circ_{yy} \times 100$	0.53	0.52	0.49	0.44	0.37	0.30	0.23	0.17	0.12
$\sigma^\circ_{\eta\eta} \times 100$	0.87	0.86	0.84	0.81	0.76	0.71	0.66	0.60	0.56

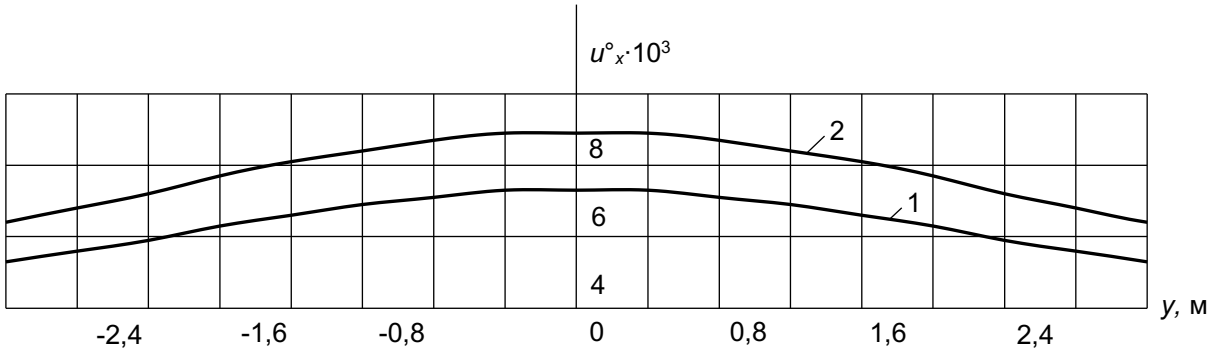

Fig. 2 Displacements u°_x at the ground surface in the xy coordinate plane

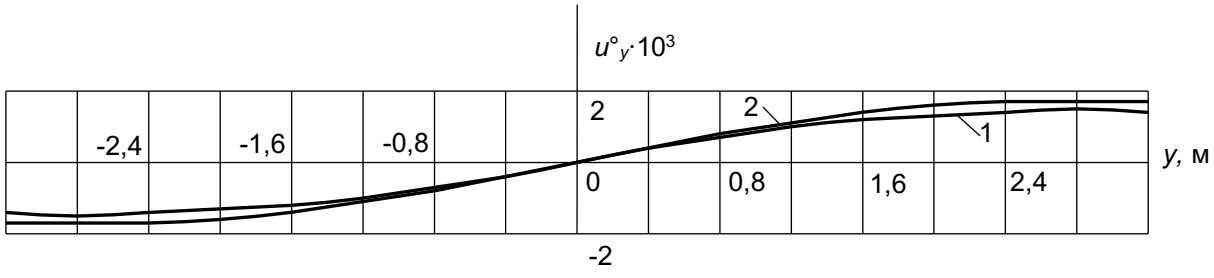

Fig. 3 Displacements u°_y at the ground surface in the xy coordinate plane

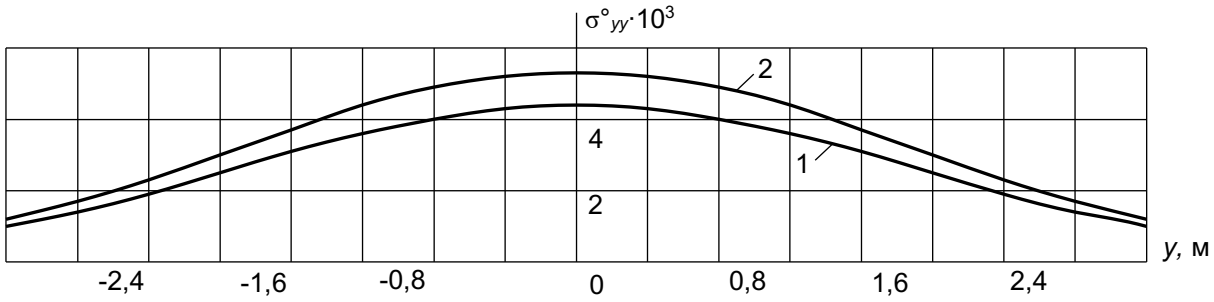

Fig. 4 Stresses σ°_{yy} at the ground surface in the *xy* coordinate plane

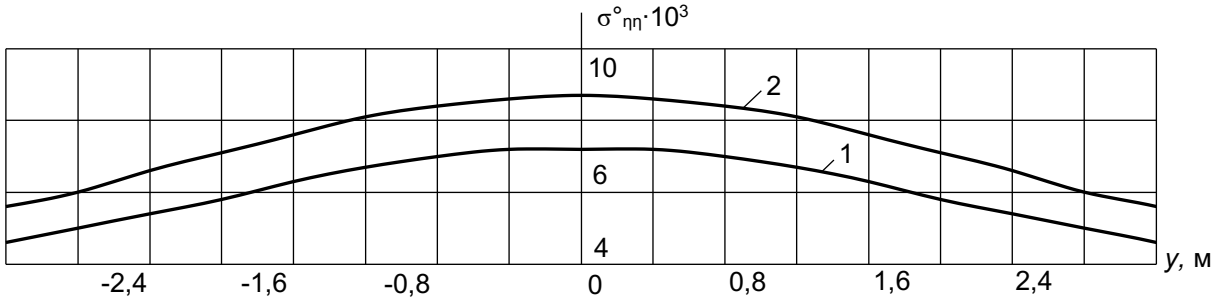

Fig. 5 Stresses $\sigma^{\circ}_{\eta\eta}$ at the ground surface in the *xy* coordinate plane in the *xy* coordinate plane

5. DISCUSSION

Analysis of the results indicates that on the inner surface of the supporting lining layer ($r = R_2$, $\eta = 0$), stresses $\sigma_{\theta\theta}$ are tensile, while stresses $\sigma_{\eta\eta}$ are compressive. The contact conditions between the lining and the surrounding rock body have a negligible impact on their numerical values, as well as on radial displacement values u_r. Radial stresses σ_{rr} corresponds to the boundary condition. On the contour of the outer surface of the supporting lining layer ($r = R_1$, $\eta = 0$) there are also tensile stresses $\sigma_{\theta\theta}$, $\sigma_{\eta\eta}$ that depend little on the contact conditions of the lining with the rock body. At the same time, the stress $\sigma_{\theta\theta}$ is approximately 2 times greater, and the stress $\sigma_{\eta\eta}$ is 3 times lower corresponding stress $\sigma_{\theta\theta}$ and $|\sigma_{\eta\eta}|$ on the contour of the inner surface of the supporting lining layer. Regardless of the contact conditions between the lining and the rock body, the stress magnitude $|\sigma_{rr}|$ on the outer contour of the concrete lining surface is almost 17 times smaller than $|\sigma_{rr}|$ on the inner contour, while the reduction in displacement values u_r is insignificant.

On the contour of the contact surface of the rock body ($r = R_1$, $\eta = 0$) the radial displacements u_r correspond to the radial displacements on the outer contour of the supporting layer surface, while the magnitudes of the stresses $|\sigma_{rr}|$, $|\sigma_{\theta\theta}|$, $|\sigma_{\eta\eta}|$ are significantly smaller (Table 2). In the case of rigid contact between the lining and the rock body, tensile stresses $\sigma_{\theta\theta}$ and compressive stresses σ_{rr}, $\sigma_{\eta\eta}$, act, while in the case of sliding contact, the stresses σ_{rr}, $\sigma_{\theta\theta}$, $\sigma_{\eta\eta}$ are compressive. In the case of rigid contact of the lining with the rock mass, the magnitude of the stress $|\sigma_{rr}|$ on the contact surface contour is higher compared to the case of sliding contact, the stresses $|\sigma_{\eta\eta}|$ are substantially lower, and the stress magnitudes $|\sigma_{\theta\theta}|$ have different signs.

With moving away from the tunnel lining, the values of rock mass SSS components attenuate. On the ground surface, in the case of rigid contact between the lining and the rock body, the displacements u_x and the stresses σ_{yy}, $\sigma_{\eta\eta}$ are lower compared to the case of sliding contact (Table 3). These components have the highest values at $y = 0$ and quickly diminish as $|y|$ increases (Fig. 2 – 5).

6. CONCLUSION

The model problem of the dynamics of a shallowly buried tunnel reinforced with a two-layer lining under the influence of a stationary transport load has been solved. Unlike similar works in which the rock body is represented as an elastic space, in this study it is represented as an elastic half-space.

The study focused on examining a shallowly embedded tunnel reinforced with a two-layer steel-concrete lining (comprising a thick inner concrete layer and a thin outer steel layer), subjected to a uniformly moving axisymmetric cylindrical compressive load. The contact between the rock body

and the lining of the tunnel was assumed to be either rigid or sliding. By using the computer program developed by the authors, SSS components were computed for the cross-sectional plane of the tunnel that passes through the middle of the moving load. An analysis of the calculation results has been conducted, from which it is established that the contact conditions between the rock body and the lining have a minor influence on the SSS of its inner layer and a significant impact on the stresses along the contact surface of the body. On the Earth's surface, displacements and stresses are lower with a rigid lining-body contact than with a sliding contact.

The developed mathematical model for shallowly embedded tunnel dynamics is recommended to design organizations in the field of metro construction and tunnel engineering. When designing a tunnel lining, it's important to consider not only the physical and mechanical properties of the materials used and the rock mass itself, but also the structural features of the tunnel, the depth at which it's embedded, and the type and speed of the transport load it will carry. The widespread introduction of high-speed transport has made the latter especially relevant. Additionally, it is worth noting that the speed of modern vehicles lies in the subsonic range and is much less than its upper limit.

7. REFERENCES

[1] Yerzhanov Zh.S. and Aitaliev Sh.M., The dynamics of tunnels and underground pipelines, Nauka, Alma-Ata, 1989, pp. 1-240.

[2] Gospodarikov A. and Thanh N.Ch., Behavior of segmental tunnel linings under the impact of earthquakes: a case study from the tunnel of Hanoi metro system, International Journal of GEOMATE, Vol. 15, No. 48, 2018, pp. 91–98.

[3] Sheng X., A Review on Modelling Ground Vibrations Generated by Underground Trains, International Journal of Rail Transportation, Vol. 7, No. 4, 2019, pp. 241–261.

[4] Lvovsky V.M., Steady-state oscillations of a cylindrical shell in an elastic medium under the action of a moving load, Sat.: Issues of ductility, Dnipropetrovsk, 1974, pp. 98-110.

[5] Pozhuev V.I., The action of a moving load on a cylindrical shell in an elastic medium, Structural Mechanics and Structural Analysis, No.1, 1978, pp. 44-48.

[6] Yang Y.B. and Hung H.H., Soil Vibrations Caused by Underground Moving Trains, Journal of Geotechnical and Geoenvironmental Engineering, Vol. 134, No. 11, 2008, pp. 1633-1644.

[7] Alekseeva L.A., Dynamics of an elastic half-space with a reinforced cylindrical cavity under moving loads, International Applied Mechanics, Vol. 45, Issue 0, 2009, pp. 75-85.

[8] Ukrainets V.N., The action of a moving load on a thick-walled shell in an elastic half-space, Bulletin of Pavlodar State University. Physics and Mathematics series., No. 4, 2010, pp. 81-87.

[9] Alekseeva L.A., Mathematical simulation of the dynamics of shallowly submerged tunnels and pipelines, Vestnik of Lobachevsky State University of Nizhni Novgorod, No. 4, Part 5, 2011, pp. 1954-1956.

[10] Coşkun İ. and Dolmaseven D., Dynamic Response of a Circular Tunnel in an Elastic Half Space, Journal of Engineering, Vol. 2017, 2017, 12 p.

[11] Yuan Z., Boström A. and Cai Y., Benchmark solution for vibrations from a moving point source in a tunnel embedded in a half-space, Journal of Sound and Vibration, Vol. 387, 2017, pp. 177-193.

[12] Zhou Sh., Dynamics of Rail Transit Tunnel Systems, Academic Press, 2019, pp 1-276.

[13] Girnis S.R. and Gorshkova L.V., The impact of normal and tangential loads on a shallow tunnel, Bulletin of L.N. Gumilyov ENU. Mathematics. Computer science. Mechanics series, Vol. 144, No. 3, 2023, pp. 12-22.

[14] Girnis S.R., Makashev K.T. and Stanevich V.T., Dynamic response of unsupported and supported cavities in an elastic half-space under moving normal and torsional loads, Bulletin of the Karaganda University. Physics series, Vol. 112, No. 4, 2023, pp. 65-75.

[15] Rakhimov M.A., Rakhimova G.M. and Suleimbekova Z.A., Modification of Concrete Railway Sleepers and Assessment of Its Bearing Capacity, International Journal of GEOMATE, Vol. 20, No. 27, 2021, pp. 40-48.